MODAL ANALYSIS OF LAMINATES BY A MIXED ASSUMED-STRAIN FINITE ELEMENT MODEL

ANTONIO CAZZANI, NICOLA LUIGI RIZZI, FLAVIO STOCHINO, AND EMILIO TURCO

Abstract. Fibre reinforced plates and shells are finding an increasing interest in engineering applications; in most cases dynamic phenomena need to be taken into account. Consequently, effective and robust computational tools are sought in order to provide reliable results for the analysis of such structural models. In this paper the mixed assumed-strain laminated plate element presented in [1], and used there for static analyses, has been extended to the dynamic realm. This model is derived within the framework of the so called First-order Shear Deformation Theory (FSDT) [2], [3]. What is peculiar in this assumed-strain finite element is that in-plane strain components are directly modeled; the corresponding stress components are deduced via constitutive law. By enforcing the equilibrium equations for each lamina, and account taken of continuity requirements, the out-of-plane shear stresses are computed and, finally, constitutive law provides the corresponding strains. The resulting global strain field depends only on a fixed number of parameters, regardless of the total number of layers. Since the proposed element is not locking-prone, even in the thin plate limit, and provides an accurate description of inter-laminar stresses, an extension to the dynamic range seems to be particularly attractive. The same kinematic assumptions will lead to the formulation of a consistent mass matrix. The element, developed in this way, has been extensively tested for several symmetric lamination sequences; comparison with available analytical solutions and with numerical results obtained by refined 3-D models are presented, too.

1. Introduction

Several theories have been developed to study the structural behavior of laminated composite plates, in particular (see Reddy [4] and references cited therein) it is possible to distinguish:

(1) Equivalent Single Layer Theories (ESL) such as: Classical Plate Lamination Theory (CLPT), which is an extension of Kirchhoff's plate theory (where shear straining is not taken into account); First-order Shear Deformation Theory (FSDT), which being an extension of Reissner-Mindlin plate theory accounts for shear strains in the simplest way (see [5, 6, 7, 8, 9]); and Higher-order Shear Deformation Theories (HSDTs), providing models able to deal with non linear shear strain distributions (see [10, 11, 12, 13, 14, 15, 16]; and also [17, 18]).
(2) Layer-wise Lamination Theory (LLT), which accounts for continuous transverse stresses at the interfaces separating dissimilar materials. It provides a more kinematically correct representation of the cross-sectional warping due to deformation of thick laminates: see, for instance, [19, 20, 21, 22].
(3) Three dimensional elasticity solutions, like those presented in [23, 24, 25].

The use of a laminate theory accounting for shear deformation is recommended for flat structures where the longitudinal elastic modulus of the lamina (often consisting of a fibre-reinforced composite) is much higher than both shear and transverse moduli. Indeed, plates made of fibre

1991 *Mathematics Subject Classification.* Primary 74H45, 74Q10, 74S05; Secondary 74K30, 74H15, 74B05, 35B27, 74S30.

Key words and phrases. Fibre reinforced material, Plates, Vibration analysis, Finite element method, Mixed variational principles.

reinforced composite materials are characterized by non negligible shear deformations in the thickness direction. FSDT theory has often been considered the best compromise between accuracy and computational cost for a wide class of applications, as it was stated, for instance, by Cen *et al.* [26]: "To date, FSDT is still considered the best compromise between the capability for prediction and computational cost for a wide class of applications". Indeed it accounts for shear deformations along the thickness in the simplest way and gives satisfactory results for a wide class of structural problems requiring only C^0 continuity for the displacement field. Its basic assumptions are: straight lines perpendicular to the midsurface before deformation remain straight after deformation but, in general, do not remain perpendicular to the midsurface after deformation. Actually these hypothesis lead to two main consequences: the assumption of constant shear stresses along the plate thickness is such that boundary conditions on the top and on the bottom surface are violated; shear correction factors must be introduced (see more details in [27, 28, 3]).

Several methods have been proposed to improve FSDT results in finite element analysis via post-processing methods (see [29] and [9]). In addition, other refined FSDT models can be found in the literature, which are based on the assumption that shear strains vary in the thickness in cylindrical bending with the same law as the shear stresses obtained by integrating the equilibrium equations ([2] and [30]). Regarding FE models it is usual to present FSDT within the framework of a displacement approach; however hybrid and mixed formulations have been proposed as well: see for example [31, 32, 33, 34].

In this paper the laminate mixed assumed-strain plate element presented in [1] has been extended to dynamics: perfect bonding between laminae and basic assumptions of FSDT theory have been considered. In-plane components of the strain tensor are interpolated and assumed to vary linearly along the thickness. The corresponding in-plane stress distribution is deduced, via constitutive law, for each lamina, whereas out-of-plane shear stresses are computed by integrating the equilibrium equations in each lamina and taking into account the interlaminar continuity requirements. By means of inverse constitutive law out-of-plane shear strain are finally obtained. A four node element is derived from a Hu–Washizu [35] three field mixed variational principle; enforcing its stationary conditions the stiffness and mass matrix of the element have been obtained. In analogy with a previously developed non-symmetric hybrid assumed-stress homogeneous plate element (see [36]) the shear strain energy turns out to be *exactly* zero in the thin plate limit, thus preventing the occurrence of locking phenomena. To test the reliability of the proposed element in dynamics applications the eigenproblem has been solved for some meaningful benchmark problems.

The organization of the rest of this paper is the following: in Section 2 the underlying theory necessary for developing the proposed finite element is carefully explained; the resulting stiffness and mass matrices (which depend only on displacement-type degrees of freedom, once strain parameters have been eliminated, by static condensation, at element level) are presented in Section 3. Two meaningful dynamic applications to cross-ply laminates, such that analytic reference solutions are available via FSDT, are shown and commented upon in Section 4; the former, which is relevant to free vibration of a cantilever laminated plate, is a typical problem, often, but not here, analysed within the framework of cylindrical bending; the latter, involving free vibrations of a simply supported square laminated plate, is a genuine 2-D bending problem. For both problem also a 3-D solution obtained by a commercial finite element code with a suitably refined mesh has been reported for comparison purposes. Finally in Section 5 conclusions are drawn and some perspective of future research investigation are illustrated.

Please cite this document as: Cazzani, Rizzi, Stochino and Turco Modal analysis of laminates by a mixed assumed-strain finite element model, Mathematics and Mechanics of Solids, 2018, Vol. 23(1) 99 –119, DOI:10.1177/1081286516666405

2. A mixed assumed-strain laminated plate model

In this Section the mechanical theory which allows to formulate in a coherent way the proposed laminated plate model will be introduced, starting from general issues and arriving at formulation details. Hence after presenting the underlying mixed variational principle, the reader will be introduced to the geometry and mechanical behavior of a typical lamina. Then gluing together a stack of laminae (under the assumption of perfect bonding) the kinematic hypotheses of a laminated plate will be put forth, and a method for computing the out-of-plane strain components will be described. Finally the introduction of suitable discretization for the field variables will lead to the complete definition of the proposed mixed assumed-strain finite element for laminated plates.

2.1. Some useful mixed variational principles.

The starting point for developing, in the framework of linear elasticity under infinitesimal strain conditions, the variational formulation of the proposed model is a three-field variational principle of the Hu-Washizu type (see [35]). For a 3-D continuum, occupying a volume Ω, bounded by a smooth surface $\partial\Omega$ composed of two non intersecting portions, namely $\partial\Omega_u$ (where displacements are prescribed) and $\partial\Omega_s$ (where traction boundary conditions must be fulfilled) the corresponding functional is:

$$\begin{aligned}\Pi_{HW}(\sigma_{ij},\varepsilon_{ij},u_i) = &\int_\Omega \left(\frac{1}{2}C_{ijmn}\varepsilon_{ij}\varepsilon_{mn} - b_i u_i\right)\mathrm{d}V - \int_\Omega \sigma_{ij}\left[\varepsilon_{ij} - \frac{1}{2}(u_{i,j}+u_{j,i})\right]\mathrm{d}V \\ &- \int_{\partial\Omega_s} f_i u_i \mathrm{d}S - \int_{\partial\Omega_u} \sigma_{ij} n_j (u_i - \overline{u}_i)\mathrm{d}S\,.\end{aligned} \tag{1}$$

In (1), where indicial notation referred to Cartesian coordinates is used, C_{ijmn}, σ_{ij}, ε_{ij}, u_i represent, respectively, the components of the fourth-order elasticity tensor, of the second-order stress and strain tensors and of the displacements vector; f_i and b_i denote, respectively, the components of the surface and body forces and, finally, $\overline{u}_i$ are prescribed displacement components, while n_i is the outward-directed unit normal to the surface of the body; moreover a comma means differentiation with reference to the corresponding coordinate. Here and in the sequel Einstein's convention implying summation of repeated indices is assumed, unless indices are written within brackets.

From the stationary condition of functional (1), provided that the stress tensor is *a priori* symmetric, namely $\sigma_{ij} - \sigma_{ji} = 0$ (thus satisfying the Angular Momentum Balance, AMB), all governing field equations in strong form can be deduced, namely

- Constitutive Law (CL): $\sigma_{ij} = C_{ijmn}\varepsilon_{mn}$;
- kinematic Compatibility Condition (CC): $\varepsilon_{ij} = \dfrac{u_{i,j}+u_{j,i}}{2}$;
- Linear Momentum Balance (LMB): $\sigma_{ij,j} + b_i = 0$,

as well as the relevant Boundary Conditions (BCs).

If Constitutive Law (CL) is *a priori* assumed, the stress components can be eliminated from (1), resulting in the following *modified* Hu-Washizu functional depending only on two fields (strains and displacements):

$$\begin{aligned}\Pi_{HW_{\mathrm{mod}\,1}}(\varepsilon_{ij},u_i) = &-\frac{1}{2}\int_\Omega C_{ijmn}\varepsilon_{ij}\varepsilon_{mn}\mathrm{d}V + \frac{1}{2}\int_\Omega \left[C_{ijmn}\varepsilon_{mn}(u_{i,j}+u_{j,i})\right]\mathrm{d}V - \int_\Omega b_i u_i \mathrm{d}V \\ &- \int_{\partial\Omega_s} f_i u_i \mathrm{d}S - \int_{\partial\Omega_u} C_{ijmn}\varepsilon_{mn} n_j (u_i - \overline{u}_i)\mathrm{d}S\,.\end{aligned} \tag{2}$$

This functional can be further modified by applying the divergence theorem to the second term on the right hand side and then simplifying the resulting boundary terms so that this alternate form of

Please cite this document as: Cazzani, Rizzi, Stochino and Turco Modal analysis of laminates by a mixed assumed-strain finite element model, Mathematics and Mechanics of Solids, 2018, Vol. 23(1) 99 –119, DOI:10.1177/1081286516666405

a modified two-fields Hu-Washizu functional is obtained:

$$\Pi_{HW_{\text{mod }2}}(\varepsilon_{ij}, u_i) = -\frac{1}{2}\int_\Omega C_{ijmn}\varepsilon_{ij}\varepsilon_{mn}\mathrm{d}V - \int_\Omega (C_{ijmn}\varepsilon_{mn,j} + b_i)u_i\mathrm{d}V + \int_{\partial\Omega_s}(C_{ijmn}\varepsilon_{mn}n_j - f_i)u_i\mathrm{d}S + \int_{\partial\Omega_u} C_{ijmn}\varepsilon_{mn}n_j\overline{u}_i\mathrm{d}S\,. \tag{3}$$

It can be easily checked that stationary conditions of both two-field functionals provide the strong form of CC and LMB (expressed in terms of strains), as well as the relevant BCs.

2.2. **Laminated plate geometry and mechanical properties.** With the term laminate plate a thin (or moderately thick) flat body is referred to, which is constituted by K layers with different mechanical characteristics, stacked one above the other and occupying the domain:

$$\Omega = \left\{(x_1, x_2, x_3) \in \mathbb{R}^3 \mid x_3 \in [-h/2, +h/2], \quad (x_1, x_2) \in \tilde{\Omega} \subset \mathbb{R}^2\right\}, \tag{4}$$

where the plane $\tilde{\Omega}$ (*i.e.* $x_3 = 0$) coincides with the middle surface of the undeformed plate, and the transverse dimension, whose thickness is h, is small compared to the other two dimensions. Layers are assumed to lie parallel to the middle surface $\tilde{\Omega}$; the typical k-th layer ($k = 1, \ldots, K$) lies between thickness coordinates h_{k-1} and h_k and is supposed to behave as orthotropic (even if extension to a monoclinic material is relatively easy to perform) with material axes oriented at an angle $\theta^{(k)}$ with reference to coordinate x_1 of the global reference system of the plate.

The whole lateral surface of the body, $\partial\Omega$, is the union of the upper and lower faces Ω^+ and Ω^- and of the lateral surface Ω^L, see Figure 1.

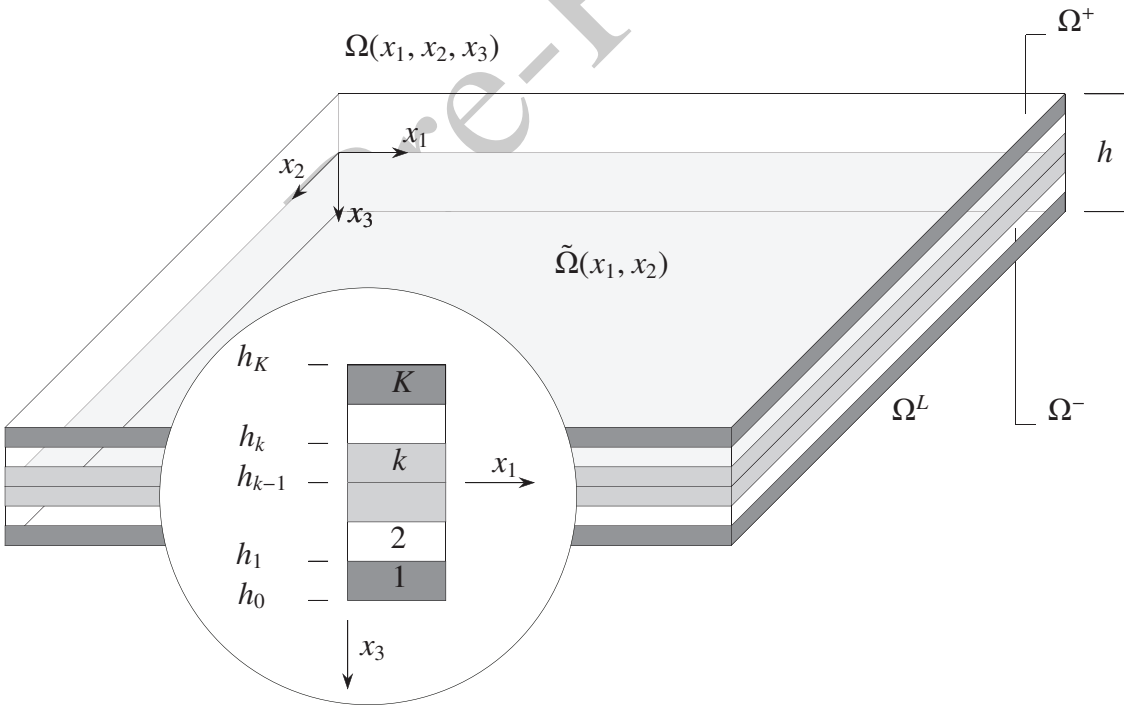

FIGURE 1. Reference system and layer numbering for a typical laminated plate.

Before discussing in detail the model kinematics, the terminology associated with the particular lamination scheme considered is here introduced. The lamination scheme of the plate will be

Please cite this document as: Cazzani, Rizzi, Stochino and Turco Modal analysis of laminates by a mixed assumed-strain finite element model, Mathematics and Mechanics of Solids, 2018, Vol. 23(1) 99 –119, DOI:10.1177/1081286516666405

denoted by

$$\theta^{(1)}/\theta^{(2)}/\theta^{(3)}/\ldots/\theta^{(k)}/\ldots/\theta^{(K)},$$

where $\theta^{(1)}$ is the orientation of the material orthotropy axis $\hat{x}_1$ of the first layer with reference to x_1, $\theta^{(2)}$ that of the second layer, and so on (see Figure 2).

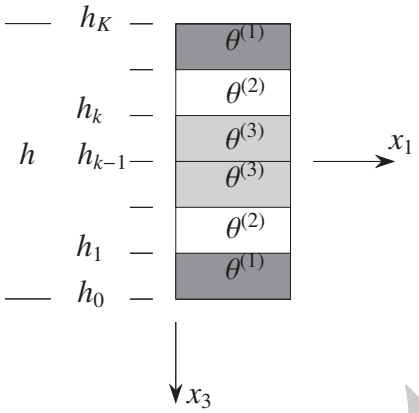

FIGURE 2. Lamination scheme for a symmetric laminate $\left[\theta^{(1)}/\theta^{(2)}/\theta^{(3)}/\theta^{(3)}/\theta^{(2)}/\theta^{(1)}\right] = \left[\theta^{(1)}/\theta^{(2)}/\theta^{(3)}\right]_S$.

A laminate is said to be *symmetric* if the layer stacking sequence, the material properties and the geometry of the layers are symmetric with reference to the midplane $\tilde{\Omega}$ of the laminate. From now on, for conciseness sake, only laminated plate satisfying a symmetric lamination scheme will be taken into account. Moreover since each lamina is supposed to be very thin, plane stress conditions are postulated.

As a consequence, once Voigt's notation is adopted for the fourth-order elastic tensor (which implies these substitutions of indices: $11 \to 1$; $22 \to 2$; $33 \to 3$; $23 \to 4$; $13 \to 5$; $12 \to 6$ the CL for the k-th lamina (when it is referred to the principal axes of orthotropy $\hat{x}_1$, $\hat{x}_2$, $\hat{x}_3 = x_3$) reads, account taken of symmetries:

$$\begin{aligned}
\hat{\sigma}_{11}^{(k)} &= C_{11}^{(k)}\hat{\varepsilon}_{11}^{(k)} + C_{12}^{(k)}\hat{\varepsilon}_{22}^{(k)} + C_{13}^{(k)}\hat{\varepsilon}_{33}^{(k)} = Q_{11}^{(k)}\hat{\varepsilon}_{11}^{(k)} + Q_{12}^{(k)}\hat{\varepsilon}_{22}^{(k)}\,,\\
\hat{\sigma}_{22}^{(k)} &= C_{12}^{(k)}\hat{\varepsilon}_{11}^{(k)} + C_{22}^{(k)}\hat{\varepsilon}_{22}^{(k)} + C_{23}^{(k)}\hat{\varepsilon}_{33}^{(k)} = Q_{12}^{(k)}\hat{\varepsilon}_{11}^{(k)} + Q_{22}^{(k)}\hat{\varepsilon}_{22}^{(k)}\,,\\
\hat{\sigma}_{33}^{(k)} &= C_{13}^{(k)}\hat{\varepsilon}_{11}^{(k)} + C_{23}^{(k)}\hat{\varepsilon}_{22}^{(k)} + C_{33}^{(k)}\hat{\varepsilon}_{33}^{(k)} = 0\,,\\
\hat{\sigma}_{12}^{(k)} &= 2C_{66}^{(k)}\hat{\varepsilon}_{12}^{(k)}\,,\\
\hat{\sigma}_{13}^{(k)} &= 2C_{55}^{(k)}\hat{\varepsilon}_{13}^{(k)}\,,\\
\hat{\sigma}_{23}^{(k)} &= 2C_{44}^{(k)}\hat{\varepsilon}_{23}^{(k)}\,,
\end{aligned} \tag{5}$$

In Eqs. (5) $Q_{11}^{(k)}$, $Q_{12}^{(k)}$, $Q_{22}^{(k)}$ are the modified elastic stiffness coefficients corresponding to plane stress conditions. They are linked to the six values of the 3-D elastic stiffness coefficients $C_{11}^{(k)}$, $C_{12}^{(k)}$, $C_{13}^{(k)}$, $C_{22}^{(k)}$, $C_{23}^{(k)}$, $C_{33}^{(k)}$ in the following way:

$$Q_{11}^{(k)} = C_{11}^{(k)} - \frac{C_{13}^{(k)2}}{C_{33}^{(k)}}, \quad Q_{12}^{(k)} = C_{12}^{(k)} - \frac{C_{13}^{(k)}C_{23}^{(k)}}{C_{33}^{(k)}}, \quad Q_{22}^{(k)} = C_{22}^{(k)} - \frac{C_{23}^{(k)2}}{C_{33}^{(k)}}. \tag{6}$$

Please cite this document as: Cazzani, Rizzi, Stochino and Turco Modal analysis of laminates by a mixed assumed-strain finite element model, Mathematics and Mechanics of Solids, 2018, Vol. 23(1) 99 –119, DOI:10.1177/1081286516666405

As Eqs. (5)–(6) show, the in-plane stress-strain behavior of the lamina is governed by four coefficients only, namely $Q_{11}^{(k)}$, $Q_{12}^{(k)}$, $Q_{22}^{(k)}$, $C_{66}^{(k)}$, and the out-of-plane one by just two, *i.e.* $C_{55}^{(k)}$ and $C_{44}^{(k)}$.

When the material orthotropy axes $\hat{x}_1$, $\hat{x}_2$ do not coincide with the reference axes x_1, x_2 these stress components need to be projected along the reference axes in order to obtain the Cartesian stress components of the lamina, namely $\sigma_{11}^{(k)}$, $\sigma_{22}^{(k)}$ etc. all referred to the global reference system. This is done in this way:

$$\sigma_{ij}^{(k)} = R_{im}^{(k)} \hat{\sigma}_{mn}^{(k)} R_{jn}^{(k)}, \tag{7}$$

where $R_{ij}^{(k)}$ are the Cartesian components of a suitable rigid rotation tensor, completely defined once the angle $\theta^{(k)}$, which axes x_1 and $\hat{x}_1$ form together, is known. In particular it results:

$$\begin{aligned} &R_{11}^{(k)} = \cos\theta^{(k)}, \quad R_{12}^{(k)} = \sin\theta^{(k)}, \quad R_{13}^{(k)} = 0, \\ &R_{21}^{(k)} = -\sin\theta^{(k)}, \quad R_{22}^{(k)} = \cos\theta^{(k)}, \quad R_{23}^{(k)} = 0, \\ &R_{31}^{(k)} = 0, \qquad R_{32}^{(k)} = 0, \qquad R_{33}^{(k)} = 1. \end{aligned} \tag{8}$$

2.3. **Kinematic assumptions of the laminated plate.** In order to develop, starting from either functional (2) or functional (3), a suitable laminated plate model, some peculiar kinematic assumptions need to be introduced, so that the 3-D problem is reduced to a 2-D one, where all variables are referred to the domain of the plate midplane surface, denoted by $\tilde{\Omega}$.

A complete and detailed description of the procedure has been already reported in [36] for the homogeneous case and in [1] for the laminated one: here, for the sake of conciseness, only a short outline is given. In what follows, all quantities endowed with superscript tilde, like $\tilde{(\cdot)}$ denote variables referred to the midplane surface of the plate, $\tilde{\Omega}$, and thus depend only on coordinates x_1, x_2.

The typical assumption of the Reissner-Mindlin theory (see [37, 38]) and FSDT is adopted: particles of the plate originally lying along a straight line, which is normal to the undeformed middle surface, remain on a straight line during deformation, but this line is no more necessarily perpendicular to the deformed middle surface. Hence, the effects of shear deformations can be taken into account.

The in-plane components, (u_1, u_2), of the displacement field vary linearly along the transverse direction of the laminated plate, while the normal component, u_3 is assumed to be constant along the x_3 axis, (see Figure 3), according to these equations:

$$u_1(x_1,x_2,x_3) = -x_3\tilde{\varphi}_1(x_1,x_2), \quad u_2(x_1,x_2,x_3) = -x_3\tilde{\varphi}_2(x_1,x_2), \quad u_3(x_1,x_2,x_3) = \tilde{u}_3(x_1,x_2). \tag{9}$$

It has to be noticed that in Eq. (9), $\tilde{\varphi}_1$ and $\tilde{\varphi}_2$ represent the rotations (in the x_1 and x_2 directions respectively) of the straight transverse line elements which are normal to the reference midplane $\tilde{\Omega}$ in the undeformed configuration; they are linked to the components of the infinitesimal rotation vector along the x_1 and x_2 axes by these equations:

$$\tilde{\varphi}_1 = -\phi_2; \qquad \tilde{\varphi}_2 = \phi_1. \tag{10}$$

As it has been outlined, for instance, by Bathe (see [39]) it is more convenient to use $\tilde{\varphi}_1$ and $\tilde{\varphi}_2$ than ϕ_1, ϕ_2 in the formulation, since both expressions of u_1 and u_2 in (9) have the same sign. Similarly to the in-plane displacement components, due to the perfect bonding between laminae, also the in-plane strain components are assumed to vary linearly with reference to the transverse direction, x_3, independently of the lamina, namely:

$$\varepsilon_{11}^{(k)} = \varepsilon_{11} = x_3\tilde{\varepsilon}_{11}(x_1,x_2), \quad \varepsilon_{22}^{(k)} = \varepsilon_{22} = x_3\tilde{\varepsilon}_{22}(x_1,x_2), \quad \varepsilon_{12}^{(k)} = \varepsilon_{12} = x_3\tilde{\varepsilon}_{12}(x_1,x_2). \tag{11}$$

Please cite this document as: Cazzani, Rizzi, Stochino and Turco Modal analysis of laminates by a mixed assumed-strain finite element model, Mathematics and Mechanics of Solids, 2018, Vol. 23(1) 99 –119, DOI:10.1177/1081286516666405

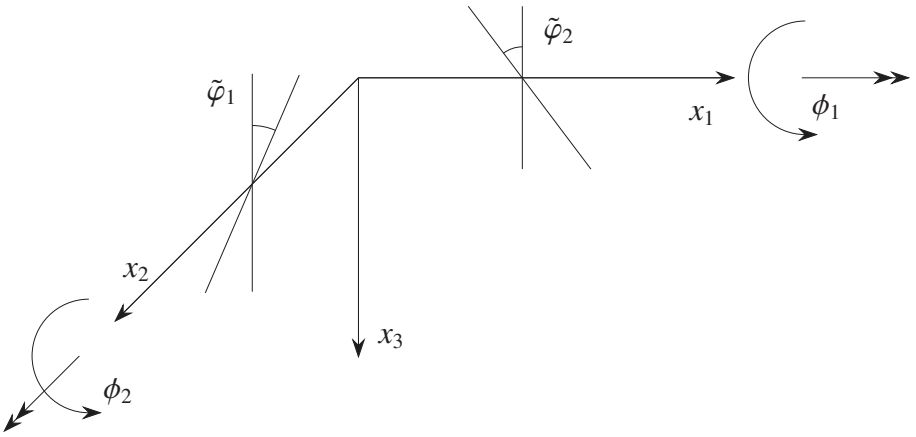

FIGURE 3. Reference system for a Reissner-Mindlin plate. Rotations of the transverse line element of the plate $\tilde{\varphi}_1$ and $\tilde{\varphi}_2$ and the corresponding Cartesian components, ϕ_1, ϕ_2 of the infinitesimal rotation vector are shown, too.

It has to be noticed that, according to Eq. (11) the *in-plane* components of the strain tensor vary linearly along the thickness, as it occurs in the classical plate theory.

As a remark, Eq. (9) which expresses the kinematics of a Reissner-Mindlin plate, and Eq. (11) are fully compatible when

$$\tilde{\varepsilon}_{11} = -\frac{\partial \tilde{\varphi}_1}{\partial x_1}, \quad \tilde{\varepsilon}_{22} = -\frac{\partial \tilde{\varphi}_2}{\partial x_2}, \quad \tilde{\varepsilon}_{12} = -\frac{1}{2}\left(\frac{\partial \tilde{\varphi}_1}{\partial x_2} + \frac{\partial \tilde{\varphi}_2}{\partial x_1}\right). \tag{12}$$

By using CL enforced at the local level for the k-th lamina, see Eqs. (5), it turns out that the *in-plane* stress components ($\sigma_{11}^{(k)}, \sigma_{22}^{(k)}, \sigma_{12}^{(k)} = \sigma_{21}^{(k)}$) vary linearly along the transverse direction of the lamina, just like in classical plate theories; however, in general, these components are discontinuous at the interface between two laminae having different orientation and/or material properties.

Out-of-plane strain components are deduced by enforcing LMB conditions for each lamina with a procedure resembling and generalizing the method used by Zhuravskii to deduce in 1855 his shear stress formula. All laminae are then stuck together in order to provide out-of-plane shear stress components which are continuous through the thickness; the corresponding shear strain are then computed by applying, layer by layer, the inverse CL. For the sake of simplicity this procedure is illustrated here only for the particular case that the material orthotropy axes of the k-th lamina are aligned with the x_1 and x_2 axes, so that $\sigma_{11}^{(k)} = \hat{\sigma}_{11}^{(k)}$, etc.; the general case where such coincidence does not occur can be handled by taking into account Eq. (7).
Indeed in such case the LMB equations for the k-th layer read, in the absence of body forces:

$$\sigma_{11,1}^{(k)} + \sigma_{12,2}^{(k)} + \sigma_{13,3}^{(k)} = 0\,, \tag{13}$$
$$\sigma_{21,1}^{(k)} + \sigma_{22,2}^{(k)} + \sigma_{23,3}^{(k)} = 0\,, \tag{14}$$
$$\sigma_{31,1}^{(k)} + \sigma_{32,2}^{(k)} = 0\,. \tag{15}$$

By taking now into account the equilibrium equations in the x_1 and x_2 directions, namely Eqs. (13))–(14), the *out-of plane* components of the stress field in the k-th layer, $\sigma_{31}^{(k)}$ and $\sigma_{32}^{(k)}$ which are supposed to satisfy *a priori* the AMB conditions, *i.e.* $\sigma_{31}^{(k)} = \sigma_{13}^{(k)}$, $\sigma_{32}^{(k)} = \sigma_{23}^{(k)}$, as it is customary in

Please cite this document as: Cazzani, Rizzi, Stochino and Turco Modal analysis of laminates by a mixed assumed-strain finite element model, Mathematics and Mechanics of Solids, 2018, Vol. 23(1) 99 –119, DOI:10.1177/1081286516666405

the classical theory of linear elasticity, can be derived explicitly. Indeed Eqs. (13)–(14) become:

$$\sigma^{(k)}_{13,3} = -x_3(\sigma^{(k)}_{11,1} + \sigma^{(k)}_{12,2})\,, \tag{16}$$

$$\sigma^{(k)}_{23,3} = -x_3(\sigma^{(k)}_{21,1} + \sigma^{(k)}_{22,2})\,. \tag{17}$$

Then by direct integration the *out-of-plane* shear components can be computed as follows:

$$\sigma^{(k)}_{13} = \sigma^{0,(k)}_{13} - \int_{-h/2}^{x_3} x_3(\sigma^{(k)}_{11,1} + \sigma^{(k)}_{12,2})\mathrm{d}x_3\,, \tag{18}$$

$$\sigma^{(k)}_{23} = \sigma^{0,(k)}_{23} - \int_{-h/2}^{x_3} x_3(\sigma^{(k)}_{21,1} + \sigma^{(k)}_{22,2})\mathrm{d}x_3\,, \tag{19}$$

where $\sigma^{0,(k)}_{13}$, $\sigma^{0,(k)}_{23}$ are integration constants which can be set by taking into account the Traction Boundary Conditions (TBCs) which require that both σ_{13} and σ_{23} must vanish on the plate bases $\Omega^{\pm}$.

So the solution in terms of out-of-plane shear stress results, for the k-th layer:

$$\sigma^{(k)}_{13} = \sigma^{0,(k)}_{13} - \frac{(x_3^2 - h_{k-1}^2)}{2}(\sigma^{(k)}_{11,1} + \sigma^{(k)}_{12,2})\,, \tag{20}$$

$$\sigma^{(k)}_{23} = \sigma^{0,(k)}_{23} - \frac{(x_3^2 - h_{k-1}^2)}{2}(\sigma^{(k)}_{21,1} + \sigma^{(k)}_{22,2})\,, \tag{21}$$

where integration constants $\sigma^{0,(k)}_{13}$ and $\sigma^{0,(k)}_{23}$ have these explicit expressions:

$$\sigma^{0,(k)}_{13} = \sum_{\ell=1}^{k-1} -\frac{(h_\ell^2 - h_{\ell-1}^2)}{2}(\sigma^{(\ell)}_{11,1} + \sigma^{(\ell)}_{12,2})\,, \tag{22}$$

$$\sigma^{0,(k)}_{23} = \sum_{\ell=1}^{k-1} -\frac{(h_\ell^2 - h_{\ell-1}^2)}{2}(\sigma^{(\ell)}_{21,1} + \sigma^{(\ell)}_{22,2})\,. \tag{23}$$

Once transverse shear stresses are known, by making use of the inverse CL the corresponding *out-of-plane* shear strain components can be evaluated: by taking into account Eq. (5), it results, for the k-th lamina:

$$\varepsilon^{(k)}_{13} = \frac{\sigma^{(k)}_{13}}{2C^{(k)}_{55}}\,, \qquad \varepsilon^{(k)}_{23} = \frac{\sigma^{(k)}_{23}}{2C^{(k)}_{44}}\,. \tag{24}$$

In this way, when Eqs. (11) and (24) are put together, an enhanced assumed strain model can be formulated. Due to the particular way of deducing it, however, only the in-plane strain components need to be directly modeled, and since they do not depend on the particular lamina, the number of strain parameters which are necessary to describe the behavior of the laminated plate is small and does not depend on the number of layers.

2.4. **Finite element discretization.** A Mixed Assumed-Strain (briefly, MAS) laminated plate element with constant thickness, which is based on the variational formulation described in Section 2.1, can be developed in the following way. Attention is focused here on a 4-noded element, which is the simpler and the least-order one, even though the same procedure can be used to generate a full family of similar N-noded, higher-order elements.

Then, given four points (the nodes) which are located on the midplane surface of the plate and are labeled 1, 2, 3, 4 (see Figure 4), a global Cartesian reference system (x_1, x_2, x_3) is taken, where

Please cite this document as: Cazzani, Rizzi, Stochino and Turco Modal analysis of laminates by a mixed assumed-strain finite element model, Mathematics and Mechanics of Solids, 2018, Vol. 23(1) 99 –119, DOI:10.1177/1081286516666405

axes x_1 and x_2 lie in the midplane and the x_3-axis is determined by the right-hand rule. Another plane natural Cartesian reference system (ξ_1, ξ_2), with $-1 \le \xi_i \le 1$ (i=1, 2) is then introduced (see, for instance [40, 41, 39]) and is related to the global one by the following relationships, which map a bi-unit square, the parent element into the real one:

$$x_i(\xi_1, \xi_2) = \sum_{\ell=1}^{4} N^\ell(\xi_1, \xi_2) x_i^\ell \,, \quad (i = 1, 2) \,, \tag{25}$$

where x_i^ℓ, (with $\ell = 1, \ldots, 4$), are the nodal coordinates of the element in the global reference system, while $N^\ell(\xi_1, \xi_2)$ are these shape functions:

$$N^\ell(\xi_1, \xi_2) = \frac{1}{4}(1 + \xi_1 \xi_1^{(\ell)})(1 + \xi_2 \xi_2^{(\ell)}) \,, \quad (\ell = 1, \ldots, 4) \,, \tag{26}$$

where, as usual, for $\ell = 1, \ldots, 4$ it results $\xi_1^{(\ell)} = -1, 1, 1, -1$ and $\xi_2^{(\ell)} = -1, -1, 1, 1$. In the frame-

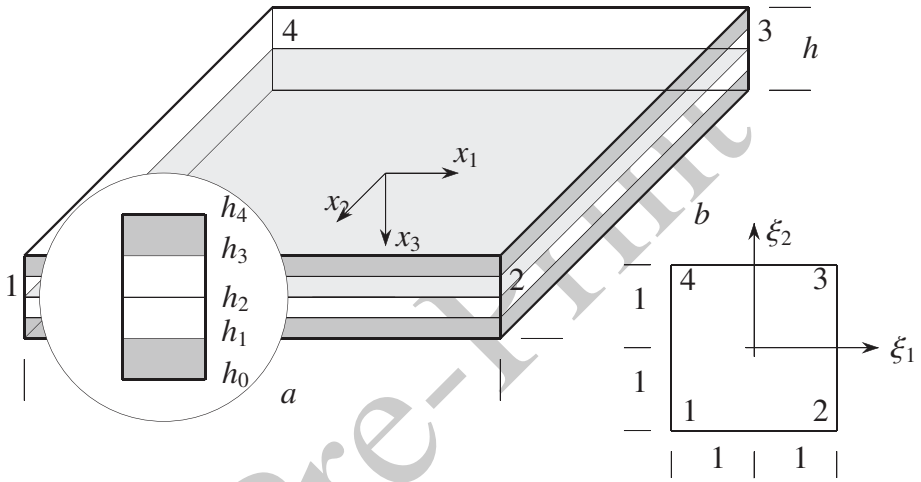

FIGURE 4. The rectangular Mixed Assumed-Strain Laminated element (MAS). In the shown example, where $K = 4$, the symmetric stacking sequence $\left[\theta^{(1)}, \theta^{(2)}, \theta^{(2)}, \theta^{(1)}\right] = \left[\theta^{(1)}, \theta^{(2)}\right]_S$ is defined by the orientation angle of each layer with reference to the x_1 axis.

work of an isoparametric approach, the components of the displacement field within the element are similarly defined as functions of the transversal displacements $\tilde{u}_3^{\,\ell}$ ($\ell = 1, \ldots, 4$) and of the rotations $\tilde{\varphi}_i^{\,\ell}$ (with $i = 1, 2$) of transverse line elements, evaluated at the four nodes of the plate. In particular, the components of the assumed displacement field depend on these nodal degrees-of-freedom (DOFs) and are expressed in terms of the same shape functions (25):

$$u_1 = -x_3 \sum_{\ell=1}^{4} N^\ell(\xi_1, \xi_2) \tilde{\varphi}_1^{\,\ell} \,, \tag{27}$$

$$u_2 = -x_3 \sum_{\ell=1}^{4} N^\ell(\xi_1, \xi_2) \tilde{\varphi}_2^{\,\ell} \,, \tag{28}$$

$$u_3 = \sum_{\ell=1}^{4} N^\ell(\xi_1, \xi_2) \tilde{u}_3^{\,\ell} \,. \tag{29}$$

Please cite this document as: Cazzani, Rizzi, Stochino and Turco Modal analysis of laminates by a mixed assumed-strain finite element model, Mathematics and Mechanics of Solids, 2018, Vol. 23(1) 99 –119, DOI:10.1177/1081286516666405

As a short-hand notation, the following generalized nodal displacement vector can be introduced:

$$\mathbf{q} = \left\{\tilde{u}_3^1, \tilde{\varphi}_1^1, \tilde{\varphi}_2^1, \tilde{u}_3^2, \tilde{\varphi}_1^2, \tilde{\varphi}_2^2, \tilde{u}_3^3, \tilde{\varphi}_1^3, \tilde{\varphi}_2^3, \tilde{u}_3^4, \tilde{\varphi}_1^4, \tilde{\varphi}_2^4\right\}^T. \tag{30}$$

The in-plane components of the strain tensor in the natural reference system ε_{ij}^* are then defined, once and for all laminae (in the sense that $\varepsilon_{ij}^{*(k)} = \varepsilon_{ij}^* \; \forall\, k$); several choices are possible: the proposed one, which depends on nine strain parameters and has been already adopted in [1], satisfies also the requirement ensuring the absence of spurious modes, see [42]. Hence these are the modeled in-plane strain components:

$$\varepsilon_{11}^* = x_3\tilde{\varepsilon}_{11}^* = x_3(\alpha_0 + \alpha_1\xi_1 + \alpha_2\xi_2)\,, \tag{31}$$

$$\varepsilon_{22}^* = x_3\tilde{\varepsilon}_{22}^* = x_3(\beta_0 + \beta_1\xi_1 + \beta_2\xi_2)\,, \tag{32}$$

$$\varepsilon_{12}^* = x_3\tilde{\varepsilon}_{12}^* = x_3(\gamma_0 + \gamma_1\xi_1^2 + \gamma_2\xi_2^2)\,. \tag{33}$$

As a consequence, in-plane extensional strain components are modeled as complete linear polynomials, while the in-plane shear strain component is defined by an incomplete quadratic polynomial. The parameters which describe through (31)–(33) the in-plane strain components can be usefully collected into this strain vector $\boldsymbol{\beta}$:

$$\boldsymbol{\beta} = \{\alpha_0, \alpha_1, \alpha_2, \beta_0, \beta_1, \beta_2, \gamma_0, \gamma_1, \gamma_2\}^T. \tag{34}$$

In order to express the Cartesian strain components $\varepsilon_{mn}^{(k)}$ of the k-th lamina, the strains defined in the natural reference system ε_{ij}^* must be transformed into the global reference system:

$$\varepsilon_{mn}^{(k)} = J_{im}\varepsilon_{ij}^* J_{jn}, \tag{35}$$

where J_{im} denote the elements of the Jacobian matrix associated to the isoparametric mapping (25).

3. Stiffness and mass matrices for modal analysis

The stiffness matrix $\mathbf{K}$ can be obtained introducing the previous interpolation fields, see Eqs. (27)–(29) and (31)–(33), into the modified Hu–Washizu functional (2) and enforcing the stationary conditions of the resulting discretized variational principle:

$$\Pi^e_{HW_{\text{mod 1}}} = -\frac{1}{2}\boldsymbol{\beta}^T\mathbf{H}_{\beta\beta}\boldsymbol{\beta} + \boldsymbol{\beta}^T\mathbf{G}\mathbf{q} - \mathbf{F}^T\mathbf{q}\,, \tag{36}$$

with:

$$\boldsymbol{\beta}^T\mathbf{H}_{\beta\beta}\boldsymbol{\beta} = \sum_{k=1}^{K}\left[\int_{\tilde{\Omega}}^{e} C_{ijmn}^{(k)}\int_{h_{k-1}}^{h_k}\varepsilon_{ij}^{(k)}\varepsilon_{mn}^{(k)}\mathrm{d}x_3\mathrm{d}A\right], \tag{37}$$

$$\boldsymbol{\beta}^T\mathbf{G}\mathbf{q} = \sum_{k=1}^{K}\left[\int_{\tilde{\Omega}}^{e} C_{ijmn}^{(k)}\int_{h_{k-1}}^{h_k}\varepsilon_{mn}^{(k)}\frac{(u_{i,j}+u_{j,i})}{2}\mathrm{d}x_3\mathrm{d}A\right], \tag{38}$$

$$\mathbf{F}^T\mathbf{q} = \sum_{k=1}^{K}\left[\int_{\tilde{\Omega}}^{e}\int_{h_{k-1}}^{h_k} b_i^{(k)}u_i\mathrm{d}x_3\mathrm{d}A\right], \tag{39}$$

where no boundary contributions survive if there is no surface loading and prescribed displacements are assumed to vanish everywhere. Referring to $\boldsymbol{\beta}$ and $\mathbf{q}$, the stationary conditions of $\Pi^e_{HW_{\text{mod 1}}}$ yield:

$$\begin{bmatrix}\mathbf{H}_{\beta\beta} & \mathbf{G}\\ \mathbf{G}^T & \mathbf{0}\end{bmatrix}\begin{Bmatrix}\boldsymbol{\beta}\\ \mathbf{q}\end{Bmatrix} = \begin{Bmatrix}\mathbf{0}\\ \mathbf{F}\end{Bmatrix}. \tag{40}$$

Please cite this document as: Cazzani, Rizzi, Stochino and Turco Modal analysis of laminates by a mixed assumed-strain finite element model, Mathematics and Mechanics of Solids, 2018, Vol. 23(1) 99 –119, DOI:10.1177/1081286516666405

Since the the assumed-strain distribution is modeled only at the element level, and is not intended to be, differently from the displacement field, continuous across the border between two adjacent elements, it is possible, by means of static condensation techniques, to eliminate $\boldsymbol{\beta}$ at the element level: in this way an equivalent displacement formulation depending only on $\mathbf{q}$ results from Eq. (40), and the following discrete equilibrium equation is obtained:

$$\mathbf{K}\mathbf{q} = \mathbf{F}, \tag{41}$$

where the equivalent stiffness matrix $\mathbf{K}$ has this expression:

$$\mathbf{K} = \mathbf{G}^T \mathbf{H}_{\beta\beta}^{-1} \mathbf{G}. \tag{42}$$

If $\rho^{(k)}$ represents the material density of the k-th layer, body forces due to inertia can be taken into account as follows:

$$b_1^{(k)} = -\rho^{(k)} \ddot{u}_1\,, \quad b_2^{(k)} = -\rho^{(k)} \ddot{u}_2\,, \quad b_3^{(k)} = -\rho^{(k)} \ddot{u}_3\,. \tag{43}$$

If Eqs. (9), and (43) are used, Eq. (39) provides $\mathbf{M}$, the mass matrix which turns out to be a consistent one; the corresponding kinetic energy, $\mathcal{T}$, is similar to that provided by a classical FSDT plate model:

$$\mathcal{T} = \frac{1}{2}\dot{\mathbf{q}}^T \mathbf{M} \dot{\mathbf{q}} = \frac{1}{2} \sum_{k=1}^{K} \left[\int_{\tilde{\Omega}}^{e} \int_{h_{k-1}}^{h_k} (\rho^{(k)} x_3^2 \dot{\tilde{\varphi}}_1^2 + \rho^{(k)} x_3^2 \dot{\tilde{\varphi}}_2^2 + \rho^{(k)} \dot{\tilde{u}}_3^2) \mathrm{d}x_3 \mathrm{d}A \right], \tag{44}$$

where the first two contributions come from rotary inertia and the last one from transversal inertia.

Once mass and stiffness matrices have been identified, it is possible to perform modal analysis by applying the standard procedure used for discrete systems (see [43]). Indeed an undamped structure modeled as a multi-DOFs system, when no external loads are applied to the unrestrained DOFs, undergoes harmonic motions. The governing equation of undamped free vibrations is:

$$\mathbf{M}\ddot{\mathbf{q}}(t) + \mathbf{K}\mathbf{q}(t) = \mathbf{0}\,, \tag{45}$$

and its solution can be easily expressed by:

$$\mathbf{q} = \hat{\mathbf{q}} \sin \omega t\,, \tag{46}$$

where $\hat{\mathbf{q}}$ is a constant, time-independent, column matrix which collects componentwise the vibration amplitude of all nodal DOFs, while ω represents the angular frequency of the resulting harmonic motion. Introducing Eq. (46)) into Eq. (45), the formulation leads to a well-known generalized eigenproblem:

$$\left[\mathbf{K} - \omega^2 \mathbf{M}\right] \hat{\mathbf{q}} = \mathbf{0}\,. \tag{47}$$

The trivial solution $\hat{\mathbf{q}} = \mathbf{0}$ of Eq. (47) corresponds to static equilibrium, while non-trivial ones exist for those particular values of $\omega_i \geq 0$, ($i = 1, \ldots, N$, where N is the total number of DOF), the natural vibration frequencies which, being the *eigenvalues* of the problem, satisfy this condition:

$$\det\left[\mathbf{K} - \omega^2 \mathbf{M}\right] = \mathbf{0}\,. \tag{48}$$

A specific vibration mode $\hat{\mathbf{q}}_i$ (the corresponding *eigenvector*) is then associated to each particular natural frequency of vibration ω_i.

Please cite this document as: Cazzani, Rizzi, Stochino and Turco Modal analysis of laminates by a mixed assumed-strain finite element model, Mathematics and Mechanics of Solids, 2018, Vol. 23(1) 99 –119, DOI:10.1177/1081286516666405

4. Applications

In order to test the performance of the FE model in the dynamic range, the relevant eigenproblem has been solved for two simple cases: a cantilever laminated plate (CLP), see Figure 5, and a simply-supported square laminated plate (SSLP), see Figure 9.

The same orthotropic material has been considered for all laminae, whose density is $\rho = 1000\ \mathrm{kg/m^3}$, but with a different orientation in the stacking sequence. The mechanical properties of the material are (see [4]): $E_1 = 25$ GPa, $E_2 = 1$ GPa, $G_{12} = 0.5$ GPa, $G_{13} = 0.5$ GPa, $G_{23} = 0.2$ GPa, $\nu_{12} = 0.25$. From these values the components of the elastic tensor C_{ij} or of the modified elastic tensor Q_{ij} in compact Voigt's notation, see Eqs. (5)–(6) can be computed, since it results:

$$\begin{array}{lll} Q_{11} = \dfrac{E_1}{1-\nu_{12}\nu_{21}}, & Q_{12} = \dfrac{E_2}{1-\nu_{12}\nu_{21}}, & Q_{22} = \dfrac{E_2}{1-\nu_{12}\nu_{21}}, \\ C_{44} = G_{23} & C_{55} = G_{13} & C_{66} = G_{12}\,. \end{array} \tag{49}$$

where elastic symmetry conditions provide $\nu_{21} = \dfrac{E_2}{E_1}\nu_{12}$. For fully 3-D elastic simulations also the following three material constants need to be specified: $E_3 = 1$ GPa, $\nu_{13} = 0.01$, $\nu_{23} = 0.25$.

4.1. Cantilever laminated plate.

The first numerical test concerns the rectangular cantilever laminated plate reported in Figure 5. The plate is assumed to be clamped on the side $x_1 = 0$ and, furthermore, a unit value for b has been assumed.

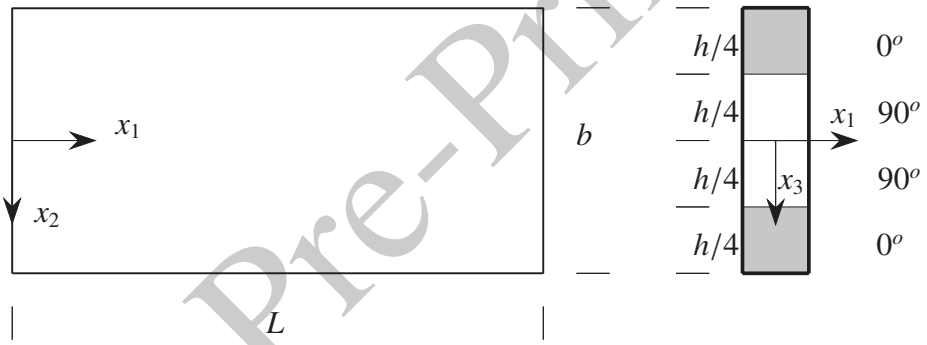

Figure 5. Cantilever laminated plate: geometry and orientation of laminae.

In Figure 6 the results concerning the relative error between the fundamental frequency produced by the MAS finite element model and FSDT for the orthotropic CLP are shown. The benchmark solution for a cantilever Timoshenko beam has been extracted from [4] and, in order to have a thorough comparison, the degrees of freedom (dofs) which are relevant to torsional rotation have been constrained. In this way the fundamental frequency of a beam could be reproduced. The relative error is plotted against the degrees of freedom. Of course, convergence is achieved by refining the mesh. Tables 1, 2 and 3 report, respectively, the first three natural frequencies, ω_1, ω_2, ω_3 (all expressed in a dimensionless form) for a laminated CLP with this stacking sequence: $[0°/90°/90°/0°] = [0°/90°]_S$. The results produced by the MAS finite element lie between those produced by FSDT and by a well refined finite element mesh created with standard displacement-based eight-noded 3-D bricks implemented in ANSYS. The dimensionless form used to express angular frequencies is the following:

$$\hat{\omega}_i = \omega_i \frac{L^2}{h}\sqrt{\frac{\rho}{E_2}}, \tag{50}$$

Please cite this document as: Cazzani, Rizzi, Stochino and Turco Modal analysis of laminates by a mixed assumed-strain finite element model, Mathematics and Mechanics of Solids, 2018, Vol. 23(1) 99 –119, DOI:10.1177/1081286516666405

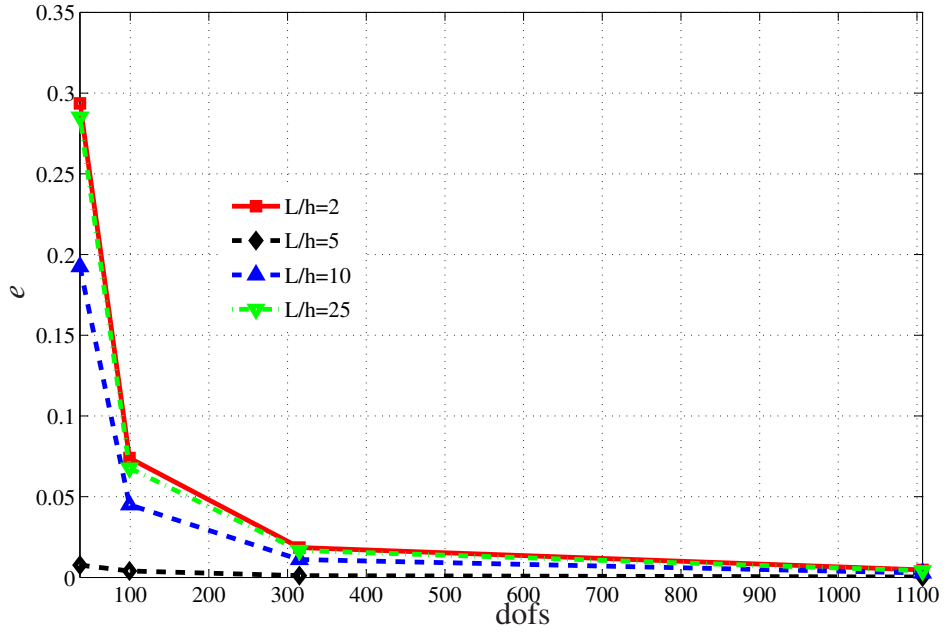

FIGURE 6. Cantilever laminated plate: relative error e (in percentage) between MAS fundamental frequency and the value provided by FSDT *vs.* number of dofs.

where L is the cantilever span and h is the total thickness of the plate.

TABLE 1. Dimensionless first natural frequency $\hat{\omega}_1$ for the cantilever laminated plate, four equal thickness layers with stacking sequence $[0°/90°]_S = [0°/90°/90°/0°]$.

L/h	mesh	MAS	FSDT	ANSYS 3D	ANSYS mesh
	5x1	2.8915			
	10x2	2.8895			
5	20x4	2.8903			
	40x8	2.8955			
	ref.	—	2.8882	2.9174	40x8x8
	5x1	3.9928			
	10x2	3.9968			
10	20x4	3.9979			
	40x8	3.9990			
	ref.	—	3.9979	4.0283	80x8x8
	5x1	4.6032			
	10x2	4.6128			
25	20x4	4.6150			
	40x8	4.6156			
	ref.	—	4.6157	4.6154	200x8x8

257

Please cite this document as: Cazzani, Rizzi, Stochino and Turco Modal analysis of laminates by a mixed assumed-strain finite element model, Mathematics and Mechanics of Solids, 2018, Vol. 23(1) 99 –119, DOI:10.1177/1081286516666405

TABLE 2. Dimensionless second natural frequency $\hat{\omega}_2$ for the cantilever laminated plate, four equal thickness layers with stacking sequence $[0°/90°]_S$ = $[0°/90°/90°/0°]$.

L/h	mesh	MAS	FSDT	ANSYS 3D	ANSYS mesh
	5x1	9.4954			
	10x2	9.2596			
5	20x4	9.2055			
	40x8	9.2118			
	ref.	—	9.1782	9.9621	40x8x8
	5x1	15.9414			
	10x2	15.5525			
10	20x4	15.4547			
	40x8	15.4376			
	ref.	—	15.4185	16.0077	80x8x8
	5x1	25.5923			
	10x2	24.9282			
25	20x4	24.7507			
	40x8	24.7066			
	ref.	—	24.6902	24.8402	200x8x8

TABLE 3. Dimensionless third natural frequency $\hat{\omega}_3$ for the cantilever laminated plate, four equal thickness layers with stacking sequence $[0°/90°]_S$ = $[0°/90°/90°/0°]$.

L/h	mesh	MAS	FSDT	ANSYS 3D	ANSYS mesh
	5x1	18.8268			
	10x2	17.5698			
5	20x4	17.2569			
	40x8	17.2220			
	ref.	—	17.1325	19.2281	40x8x8
	5x1	34.6240			
	10x2	32.2894			
10	20x4	31.6809			
	40x8	31.5465			
	ref.	—	31.4693	33.2506	80x8x8
	5x1	64.4380			
	10x2	59.8342			
25	20x4	58.5561			
	40x8	58.2353			
	ref.	—	58.1220	58.9009	200x8x8

Another test aimed at evaluating how frequencies corresponding to different mode shapes vary as a function of layer thickness has been performed on the same CLP. By changing the thickness of the outer layers (those oriented at 0°), h_{outer}, and that of the inner ones (those oriented at 90°), h_{inner},

Please cite this document as: Cazzani, Rizzi, Stochino and Turco Modal analysis of laminates by a mixed assumed-strain finite element model, Mathematics and Mechanics of Solids, 2018, Vol. 23(1) 99 –119, DOI:10.1177/1081286516666405

in such a way that the total thickness of the plate is kept constant, $h = h_{\text{outer}} + h_{\text{inner}}$, a sensitivity analysis of the modes frequencies has been developed for the CLP. In this case, torsional DOFs have not been restrained. Results, which are shown in Figure 8, are expressed as a function of the dimensionless parameter $\chi = h_{\text{outer}}/h$, *i.e.* the ratio of thickness of outer layers to the total one, in the range $0.05 \leq \chi \leq 0.80$.

In particular the two cases of a thick plate ($L/h = 20$), see Figure 8(a), and of a thin one ($L/h = 100$), see Figure 8(b), have been considered. It is patent that among the first vibration modes there are four purely flexural ones and two torsional modes (see for instance Figure 7). The general trend is that an increase of the outer layer thickness (which occurs when χ increases) produces an increase of the cantilever stiffness in bending and thus flexural modes turn out to exhibit higher frequencies. Such an effect is less apparent in the case of torsional modes and this explains why some crossing of mode shapes is observed.

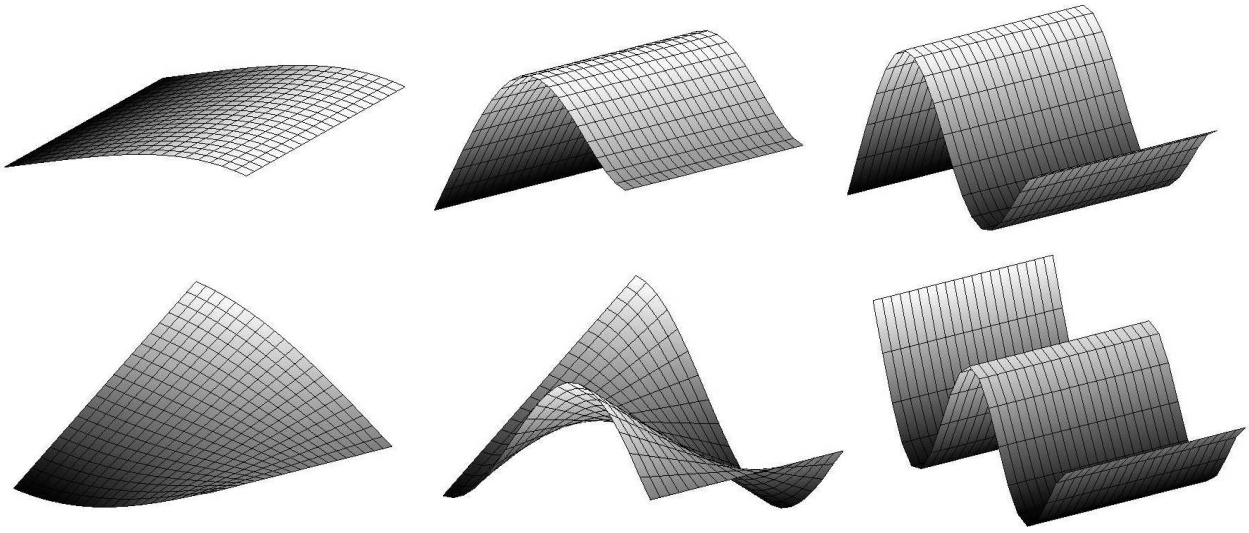

FIGURE 7. Mode shapes corresponding to the first natural frequencies of the CLP in the case $L/h = 20$ (thick plate) and $\chi = 0.10$.

4.2. **Simply-supported square laminated plate.** The second numerical test concerns a simply-supported square laminated plate reported in Figure 9. Hard boundary conditions have been assumed. In Figure 10 the results in terms of relative error between the fundamental frequency provided by MAS finite element and the analytic solution given by FSDT are depicted for the SSLP problem, again with a symmetric stacking sequence $[0°/90°]_S = [0°/90°/90°/0°]$, corresponding to a typical *cross-ply* laminate. The reference solution has been taken from [4]. As in the previous case of CLP, the relative error is plotted against the number of degrees of freedom. Also in this case convergence is achieved with mesh refinement. In Tables 4, 5 and 6 the first three natural frequencies for SSLP are reported, again in dimensionless form for the same stacking sequence. MAS results fall between those provided by FSDT and by a well refined finite element mesh based on ANSYS eight-noded 3-D bricks.

Also in this case, the sensitivity of vibration modes to changes in the thickness of the outer layers, as it has been done previously for the CLP problem, has been investigated: again the total thickness of the plate has been kept constant, and the outer layers thickness is expressed by the dimensionless parameter χ, in the range $0.05 \leq \chi \leq 0.80$. Results are reported in Figure 11: on the

Please cite this document as: Cazzani, Rizzi, Stochino and Turco Modal analysis of laminates by a mixed assumed-strain finite element model, Mathematics and Mechanics of Solids, 2018, Vol. 23(1) 99 –119, DOI:10.1177/1081286516666405

TABLE 4. Dimensionless first natural frequency $\hat{\omega}_1$ for the SSLP, four equal thickness layers with stacking sequence $[0°/90°]_S = [0°/90°/90°/0°]$.

L/h	mesh	MAS	FSDT	ANSYS 3D	ANSYS mesh
	5x5	8.1549			
	10x10	8.0361			
5	20x20	8.0127			
	40x40	8.0314			
	ref.	—	8.0489	7.5879	40x40x8
	5x5	11.8033			
	10x10	11.6088			
10	20x20	11.5589			
	40x40	11.5507			
	ref.	—	11.5876	11.2871	80x80x8
	5x5	14.7457			
	10x10	14.4519			
25	20x20	14.3763			
	40x40	14.3574			
	ref.	—	14.3667	14.2699	200x200x8

TABLE 5. Dimensionless second natural frequency $\hat{\omega}_2$ for the SSLP, four equal thickness layers with stacking sequence $[0°/90°]_S = [0°/90°/90°/0°]$.

L/h	mesh	MAS	FSDT	ANSYS 3D	ANSYS mesh
	5x5	15.5995			
	10x10	14.8076			
5	20x20	14.6419			
	40x40	14.7111			
	ref.	—	14.6190	14.0285	40x40x8
	5x5	23.2134			
	10x10	21.8575			
10	20x20	21.5219			
	40x40	21.4625			
	ref.	—	21.5532	21.1549	80x80x8
	5x5	28.9314			
	10x10	27.0583			
25	20x20	26.5921			
	40x40	26.4768			
	ref.	—	26.5036	26.3293	200x200x8

top they are plotted for the case of a thick plate ($L/h = 10$) and on the bottom those for a thin plate ($L/h = 100$). The selected vibration modes of the oscillating plate are shown in Figure 12 for the thin plate ($L/h = 100$) having $\chi = 0.1$. It can be noted that a variation of χ yields some crossing

Please cite this document as: Cazzani, Rizzi, Stochino and Turco Modal analysis of laminates by a mixed assumed-strain finite element model, Mathematics and Mechanics of Solids, 2018, Vol. 23(1) 99 –119, DOI:10.1177/1081286516666405

TABLE 6. Dimensionless third natural frequency $\hat{\omega}_3$ for the SSLP, four equal thickness layers with stacking sequence $[0°/90°]_S = [0°/90°/90°/0°]$.

L/h	mesh	MAS	FSDT	ANSYS 3D	ANSYS mesh
	5x5	15.7093			
	10x10	15.0154			
5	20x20	14.8509			
	40x40	14.8524			
	ref.	—	14.8656	14.0363	40x40x8
	5x5	28.0603			
	10x10	26.6476			
10	20x20	26.2853			
	40x40	26.2089			
	ref.	—	26.2562	25.6185	80x80x8
	5x5	48.1793			
	10x10	44.9037			
25	20x20	44.0649			
	40x40	43.8554			
	ref.	—	43.8571	43.5543	200x200x8

of flexural modes which are related to the bending stiffness in the cross-direction direction. Also in this case, the same variation is less evident for the torsional mode.

5. Concluding remarks and future perspectives

The presented Mixed Assumed-Strain finite element model, which has been already shown, see [1], to be locking-free has proven to be a powerful tool for dynamic analysis. Even with a limited number of dofs the fundamental frequency of a laminated plate structure can be computed with a small relative error (see Figures 6 and 10).

Furthermore, useful results concerning sensitivity analysis of the stacking sequence have been obtained and have been interpreted by taking into account how the thickness of each layer may affect modal analysis. Indeed the present form of the FE model is capable, in principle, of effectively managing any symmetric stacking sequence of laminae, and not only the cross-ply ones, as it occurs in both examples presented here. Further developments are planned in the future, like extending the formulation to encompass laminated plates with non symmetric stacking sequences, too. A subsequent step that the authors want to perform is introducing into the model a delamination having a known shape, in order to study how it affects mode frequencies and the relevant mode shapes.

Future perspectives of this research line mainly concern:

(1) curved structures, such as arches and shells, using the effectiveness of NURBS interpolation, see for example [44, 45, 46, 47, 48, 49, 50] and the references reported therein;
(2) reconstruction of the whole spectrum by using the guidelines reported in [51, 52, 53];
(3) damage detection, particularly important for aerospace structure, for example by using the method reported in [54, 55, 56, 57] or the numerical tools described in the review paper [58];

Please cite this document as: Cazzani, Rizzi, Stochino and Turco Modal analysis of laminates by a mixed assumed-strain finite element model, Mathematics and Mechanics of Solids, 2018, Vol. 23(1) 99 –119, DOI:10.1177/1081286516666405

(4) fracture problems, somewhat common for laminated, could be treated using the models which are well-described in [59, 60];
(5) nonlinear behavior of laminated beams, particularly those concerning buckling phenomena, following the guidelines described, for example, in [61, 62, 63, 64, 65, 66, 67, 68, 69, 70];
(6) pantographic structures such as those described in [71, 72, 73, 74, 75, 76, 77] for homogeneous material could be made more versatile if each lattice element is imagined to be made by a laminate;
(7) huge and innovative structures, such as the one described in [78, 79], which require a precise vibration control could take advantage from both the use of laminates and the effectiveness of refined computational tool such as that described here.
(8) nonlinear dynamic behavior of curved beams, see [80], and of beams under impact and blast loading, see [81, 82].

Acknowledgement

This research has been partially funded by MIUR, the Italian Ministry of Education, University and Research under grant PRIN 2010-2011 (project 2010MBJK5B – *Dynamic, Stability and Control of Flexible Structures*); such support is gratefully acknowledged.

References

[1] A. Cazzani, E. Garusi, A. Tralli, and S.N. Atluri. A four-node hybrid assumed-strain finite element for laminated composite plates. *Computer, Materials & Continua*, 2:23–38, 2005.
[2] F. Auricchio and E. Sacco. Refined first-order shear deformation theory models for composite laminates. *Journal of Applied Mechanics*, 70:381–390, 2003.
[3] M. Savoia, F. Laudiero, and A. Tralli. A two-dimensional theory for the analysis of laminated plates. *Computational Mechanics*, 14:38–51, 1994.
[4] J. N. Reddy. *Mechanics of laminated composite plates and shells — Theory and analysis*. CRC Press, Boca Raton, FL, 2nd edition, 2004.
[5] P. C. Yang, C. H. Norris, and Y. Stavsky. Elastic wave propagation in heterogeneous plates. *International Journal of Solids and Structures*, 2:665–684, 1966.
[6] J. M. Whitney and N. J. Pagano. Shear deformation in heterogeneous anisotropic plates. *Journal of Applied Mechanics ASME*, 37:1031–1036, 1970.
[7] R. Rolfes and K. Rohwer. Improved transverse shear stresses in composite finite elements based on first order shear deformation theory. *Composite Structures*, 40:51–60, 1997.
[8] R. Rolfes, K. Rohwer, and M. Ballerstaedt. Efficient linear transverse normal stress analysis of layered composite plates. *Computers & Structures*, 68:643–652, 1998.
[9] W. Yu, D.H. Hodges, and V.V. Volovoi. Asymptotically accurate 3-d recovery from reissner-like composite plate finite elements. *Computers & Structures*, 81:439–454, 2003.
[10] V. E. Chepiga. Refined theory of multilayered shells. *Soviet Applied Mechanics*, 12:1127–1130, 1976. English translation from *Prikladnaia mekhanika*, vol. 12, pp. 45–49.
[11] K. H. Lo, R. M. Christensen, and E. M. Wu. A higher-order theory of plate deformation: Part 2, laminated plates. *Journal of Applied Mechanics ASME*, 44:669–676, 1977.
[12] J. N. Reddy. A simple higher-order theory for laminated composite plates. *Journal of Applied Mechanics ASME*, 51:745–752, 1984.
[13] B. N. Pandya and T. Kant. Flexure analysis of laminated composites using refined higher-order C^0 plate bending elements. *Computer Methods in Applied Mechanics and Engineering*, 66:173–198, 1988.
[14] T. Yoda and S. N. Atluri. Post-buckling analysis of stiffened laminated composite panels, using a higher-order shear deformation theory. *Computational Mechanics*, 9:390–404, 1992.
[15] Y-K. Yong and Y. Cho. Higher-order, partial hybrid stress, finite element formulation for laminated plate and shell analysis. *Computers & Structures*, 57:817–827, 1995.
[16] P. Gaudenzi, A. Mannini, and R. Carbonaro. Multi-layer higher order finite elements for the analysis of free-edge stresses in composite laminates. *International Journal for Numerical Methods in Engineering*, 41:851–873, 1998.

Please cite this document as: Cazzani, Rizzi, Stochino and Turco Modal analysis of laminates by a mixed assumed-strain finite element model, Mathematics and Mechanics of Solids, 2018, Vol. 23(1) 99 –119, DOI:10.1177/1081286516666405

[17] V. V. Poniatovskii. Theory for plates of medium thickness. *PMM*, 26:478–486, 1962. English translation from *Prikladnaia Matematika i Mekhanika*, vol. 26, pp. 335–341.

[18] P. Cicala. Consistent approximations in shell theory. *Journal of the Engineering Mechanics Division ASCE*, 88:45–74, 1962.

[19] J. N. Reddy. A generalization of two-dimensional theories of laminated composite plates. *Communications in Applied Numerical Methods*, 3:173–180, 1987.

[20] M. Di Sciuva. An improved shear deformation theory for moderately thick multi-layered anisotropic shells and plates. *Journal of Applied Mechanics*, 54:589–596, 1987.

[21] D. H. Robbins and J. N. Reddy. Modeling of thick composites using a layerwise laminate theory. *International Journal for Numerical Methods in Engineering*, 36:655–677, 1993.

[22] P. Bisegna and E. Sacco. A layer-wise laminate theory rationally deduced from the three-dimensional elasticity. *Journal of Applied Mechanics ASME*, 64:538–545, 1997.

[23] N. J. Pagano. Exact solutions for rectangular bidirectional composites and sandwich plates. *Journal of Composite Materials*, 4:20–34, 1970.

[24] N. J. Pagano and S. J. Hatfield. Elastic behavior of multilayered bidirectional composites. *AIAA Journal*, 10:931–933, 1972.

[25] W. Liou and C. T. Sun. A three-dimensional hybrid stress isoparametric element for the analysis of laminated composite plates. *Computers & Structures*, 25:241–249, 1987.

[26] S. Cen, Y. Long, and Z. Yao. A new hybrid-enhanced displacement-based element for the analysis of laminated composite plates. *Computers & Structures*, 80:819–833, 2002.

[27] J. M. Whitney. Shear correction factors for orthotropic laminates under static load. *Journal of Applied Mechanics ASME*, 40:302–304, 1973.

[28] S. Vlachoutsis. Shear correction factors for plates and shells. *International Journal for Numerical Methods in Engineering*, 33:1537–1552, 1992.

[29] A.K. Noor and W.S. Burton. Assessment of computational models for multilayered anisotropic plates. *Composite Structures*, 14:223–265, 1990.

[30] Y. Qi and N.F. Knight. A refined first-order shear-deformation theory and its justification by plane strain bending problem of laminated plates. *Computers & Structures*, 33:49–64, 1996.

[31] S. T. Mau, P. Tong, and T. H. H. Pian. Finite element solutions for laminated plates. *Journal of Composite Materials*, 6:304–311, 1972.

[32] R. L. Spilker, O. Orringer, and E. A. Witmer. Use of the hybrid-stress finite-element model for the static and dynamic analysis of composite plates and shell. Technical Report ASRL TR 181–2, MIT, 1976.

[33] R. L. Spilker and N. I. Munir. A hybrid-stress quadratic serendipity displacement Mindlin plate bending element. *Computers & Structures*, 12:11–21, 1980.

[34] R. L. Spilker. Hybrid-stress eight-node element for thin and thick multilayered laminated plates. *International Journal for Numerical Methods in Engineering*, 18:801–828, 1982.

[35] K. Washizu. *Variational methods in elasticity and plasticity*. Pergamon Press, Oxford, 3rd edition, 1982.

[36] E. Garusi, A. Cazzani, and A. Tralli. An unsymmetric stress formulation for Reissner-Mindlin plates: a simple and locking-free hybrid rectangular element. *International Journal of Computational Engineering Science*, 5:589–618, 2004.

[37] E. Reissner. The effect of transverse shear deformation on the bending of elastic plates. *Journal of Applied Mechanics ASME*, 12:69–77, 1945.

[38] R. D. Mindlin. Influence of rotatory inertia and shear on flexural motions of isotropic elastic plates. *Journal of Applied Mechanics ASME*, 18:31–38, 1951.

[39] K. J. Bathe. *Finite element procedures*. Prentice Hall, Englewood Cliffs, NJ, 2nd edition, 1996.

[40] O. C. Zienkiewicz and R. L. Taylor. *The finite element method*. McGraw-Hill, New York, 4th edition, 1991.

[41] T. J. R. Hughes. *The finite element method — Linear static and dynamic finite element analysis*. Prentice Hall, Englewood Cliffs, NJ, 1st edition, 1987.

[42] A. Cazzani and S. N. Atluri. Four-noded mixed finite elements, using unsymmetric stresses, for linear analysis of membranes. *Computational Mechanics*, 11:229–251, 1993.

[43] R. W. Clough and J. Penzien. *Dynamics of Structures*. McGraw-Hill, New York, 1975.

[44] A. Cazzani, M. Malagù, and E. Turco. Isogeometric analysis of plane curved beams. *Mathematics and Mechanics of Solids*, 21(5):562–577, 2016.

Please cite this document as: Cazzani, Rizzi, Stochino and Turco Modal analysis of laminates by a mixed assumed-strain finite element model, Mathematics and Mechanics of Solids, 2018, Vol. 23(1) 99 –119, DOI:10.1177/1081286516666405

[45] A. Cazzani, M. Malagù, and E. Turco. Isogeometric analysis: a powerful numerical tool for the elastic analysis of historical masonry arches. *Continuum Mechanics and Thermodynamics*, 28(1):139–156, 2016.
[46] A. Cazzani, M. Malagù, E. Turco, and F. Stochino. Constitutive models for strongly curved beams in the frame of isogeometric analysis. *Mathematics and Mechanics of Solids*, 21(2):182–209, 2016.
[47] A. Bilotta, G. Formica, and E. Turco. Performance of a high–continuity finite element in three–dimensional elasticity. *International Journal for Numerical Methods in Biomedical Engineering*, 26:1155–1175, 2010.
[48] L. Greco and M. Cuomo. B-Spline interpolation of Kirchhoff–Love space rods. *Computer Methods in Applied Mechanics and Engineering*, 256:251–269, 2013.
[49] L. Greco and M. Cuomo. An implicit G^1 multi patch B-spline interpolation for Kirchhoff-Love space rod. *Computer Methods in Applied Mechanics and Engineering*, 269:173–197, 2014.
[50] L. Greco and M. Cuomo. An isogeometric implicit G1 mixed finite element for Kirchhoff space rods. *Computer Methods in Applied Mechanics and Engineering*, 298:325–349, 2016.
[51] A. Cazzani, F. Stochino, and E. Turco. On the whole spectrum of Timoshenko beams. Part I: a theoretical revisitation. *Zeitschrift für Angewandte Mathematik und Physik*, doi: 10.1007/s00033-015-0592-0:1–30, 2016.
[52] A. Cazzani, F. Stochino, and E. Turco. On the whole spectrum of Timoshenko beams. Part II: further applications. *Zeitschrift für Angewandte Mathematik und Physik*, doi: 10.1007/s00033-015-0596-9:1–21, 2016.
[53] A. Cazzani, F. Stochino, and E. Turco. An analytical assessment of finite elements and isogeometric analysis of the whole spectrum of Timoshenko beams. *Zeitschrift für Angewandte Mathematik und Mechanik*, doi: 10.1002/zamm.201500280:1–25, 2016.
[54] G. Alessandrini, A. Bilotta, G. Formica, A. Morassi, E. Rosset, and E. Turco. Numerical size estimates of inclusions in elastic bodies. *Inverse Problems*, 21:133–151, 2005.
[55] G. Alessandrini, A. Bilotta, G. Formica, A. Morassi, E. Rosset, and E. Turco. Evaluating the volume of a hidden inclusion in an elastic body. *Journal of Computational and Applied Mathematics*, 198(2):288–306, 2007.
[56] G. Alessandrini, A. Bilotta, A. Morassi, and E. Turco. Computing volume bounds of inclusions by EIT measurements. *Journal of Scientific Computing*, 33(3):293–312, 2007.
[57] E. Turco. Identification of axial forces on statically indeterminate pin–jointed trusses by a nondestructive mechanical test. *The Open Civil Engineering Journal*, 7:50–57, 2013.
[58] E. Turco. Tools for the numerical solution of inverse problems in structural mechanics: review and research perspectives. *European Journal of Environmental and Civil Engineering*, doi: 10.1080/19648189.2015.1134673:1–46, 2016.
[59] F. dell'Isola, U. Andreaus, and L. Placidi. At the origins and in the vanguard of peridynamics, non-local and higher-gradient continuum mechanics: An underestimated and still topical contribution of Gabrio Piola. *Mathematics and Mechanics of Solids*, 20(8):887–928, 2015.
[60] F. dell'Isola, A. Della Corte, R. Esposito, and L. Russo. Some cases of unrecognized transmission of scientific knowledge: from antiquity to Gabrio Piola's peridynamics and generalized continuum theories. In H. Altenbach and S. Forest, editors, *Generalized Continua as Models for Classical and Advanced Materials*, pages 77–128. Springer International Publishing, Cham, 2016.
[61] S. Gabriele, N. L. Rizzi, and V. Varano. On the imperfection sensitivity of thin-walled frames. In B. H. V. Topping, editor, *Proceedings of the Eleventh International Conference on Computational Structures Technology*, volume 99, doi: 10.4203/ccp.99.15, Stirlingshire, UK, 2012. Civil-Comp Press.
[62] M. Pignataro, G. Ruta, N. L. Rizzi, and V. Varano. Effects of warping constraints and lateral restraint on the buckling of thin-walled frames. In *ASME International Mechanical Engineering Congress and Exposition*, volume 10, pages 803–810, 2010.
[63] N. Rizzi, V. Varano, and S. Gabriele. Initial postbuckling behavior of thin-walled frames under mode interaction. *Thin–Walled Structures*, 68:124–134, 2013.
[64] S. Gabriele, N. Rizzi, and V. Varano. A 1D higher gradient model derived from Koiter's shell theory. *Mathematics and Mechanics of Solids*, 6, 2014.
[65] H. AminPour and N. Rizzi. A one-dimensional continuum with microstructure for single-wall carbon nanotubes bifurcation analysis. *Mathematics and Mechanics of Solids*, 21(2):168–181, 2016.
[66] S. Gabriele, N. L. Rizzi, and V. Varano. A 1D nonlinear TWB model accounting for in plane cross-section deformation. *International Journal of Solids and Structures*, 94–95:170–178, 2016.
[67] H. AminPour and N. L. Rizzi. On the continuum modelling of carbon nano tubes. In J. Kruis, Y. Tsompanakis, and B.H.V. Topping, editors, *Proceedings of the Fifteenth International Conference on Civil, Structural and*

Please cite this document as: Cazzani, Rizzi, Stochino and Turco Modal analysis of laminates by a mixed assumed-strain finite element model, Mathematics and Mechanics of Solids, 2018, Vol. 23(1) 99 –119, DOI:10.1177/1081286516666405

Environmental Engineering Computing, volume 108, doi:10.4203/ccp.108.240, Stirlingshire, UK, 2015. Civil-Comp Press.

[68] S. Gabriele, N. L. Rizzi, and V. Varano. A one-dimensional nonlinear thin walled beam model derived from Koiter shell theory. In B.H.V. Topping and P. Iványi, editors, *Proceedings of the Twelfth International Conference on Computational Structures Technology*, volume doi:10.4203/ccp.106.156, Stirlingshire, UK, 2014. Civil-Comp Press.

[69] H. AminPour, N. L. Rizzi, and G. Salerno. A one-dimensional beam model for single-wall carbon nano tube column buckling. In B.H.V. Topping and P. Iványi, editors, *Proceedings of the Twelfth International Conference on Computational Structures Technology*, volume 106, doi:10.4203/ccp.106.155, Stirlingshire, UK, 2014. Civil-Comp Press.

[70] N. L. Rizzi and V. Varano. On the postbuckling analysis of thin-walled frames. In B.H.V. Topping and Y. Tsompanakis, editors, *Proceedings of the 13th International Conference on Civil, Structural and Environmental Engineering Computing*, volume doi:10.4203/ccp.96.43, Stirlingshire, UK, 2011. Civil-Comp Press.

[71] F. dell'Isola, D. Steigmann, and A. Della Corte. Synthesis of fibrous complex structures: Designing microstructure to deliver targeted macroscale response. *Applied Mechanics Reviews*, 67(6):060804, 2015.

[72] I. Giorgio, R. Grygoruk, F. dell'Isola, and D. J. Steigmann. Pattern formation in the three-dimensional deformations of fibered sheets. *Mechanics Research Communications*, 69:164–171, 2015.

[73] F. dell'Isola, I. Giorgio, M. Pawlikowski, and N. L. Rizzi. Large deformations of planar extensible beams and pantographic lattices: Heuristic homogenisation, experimental and numerical examples of equilibrium. *Proceedings of the Royal Society of London A: Mathematical, Physical and Engineering Sciences*, 472(2185), 2016.

[74] D. Scerrato, I. Giorgio, and N. L. Rizzi. Three-dimensional instabilities of pantographic sheets with parabolic lattices: numerical investigations. *Zeitschrift für Angewandte Mathematik und Physik*, 67(3):1–19, 2016.

[75] D. Scerrato, I. A. Zhurba Eremeeva, T. Lekszycki, and N. L. Rizzi. On the effect of shear stiffness on the plane deformation of linear second gradient pantographic sheets. *Zeitschrift für Angewandte Mathematik und Mechanik*, doi: 10.1002/zamm.201600066, 2016.

[76] E. Turco, F. dell'Isola, A. Cazzani, and N. L. Rizzi. Hencky-type discrete model for pantographic structures: numerical comparison with second gradient continuum models. *Zeitschrift für Angewandte Mathematik und Physik*, 67(4):1–28, 2016.

[77] E. Turco, M. Golaszewski, A. Cazzani, and N. L. Rizzi. Large deformations induced in planar pantographic sheets by loads applied on fibers: experimental validation of a discrete Lagrangian model. *Mechanics Research Communications*, 76:51–56, 2016.

[78] F. Buffa, A. Cazzani, A. Causin, S. Poppi, G. M. Sanna, M. Solci, F. Stochino, and E. Turco. The Sardinia Radio Telescope: a comparison between close range photogrammetry and FE models. *Mathematics and Mechanics of Solids*, doi: 10.1177/1081286515616227:1–22, 2015.

[79] F. Stochino, A. Cazzani, S. Poppi, and E. Turco. Sardinia Radio Telescope finite element model updating by means of photogrammetric measurements. *Mathematics and Mechanics of Solids*, doi: 10.1177/1081286515616046:1–17, 2015.

[80] A. Cazzani, N. Wagner, P. Ruge, and F. Stochino. Continuous transition between traveling mass and traveling oscillator using mixed variables. *International Journal of Non-Linear Mechanics*, 66:82–95, 2015.

[81] M. Acito, F. Stochino, and S. Tattoni. Structural response and reliability analysis of RC beam subjected to explosive loading. *Applied Mechanics and Materials*, 82:434–439, 2011.

[82] F. Stochino. RC beams under blast load: Reliability and sensitivity analysis. *Engineering Failure Analysis*, 66:544–565, 2016.

Department of Civil, Environmental Engineering and Architecture (DICAAR), University of Cagliari, Italy
Email address: antonio.cazzani@unica.it

Department of Architecture, Roma Tre University, Italy
Email address: nicolaluigi.rizzi@uniroma3.it

Department of Civil, Environmental Engineering and Architecture (DICAAR), University of Cagliari, Italy
Email address: fstochino@unica.it

Department of Architecture, Design and Urban Planning (DADU), University of Sassari, Italy
Email address, corresponding author: emilio.turco@uniss.it

Please cite this document as: Cazzani, Rizzi, Stochino and Turco Modal analysis of laminates by a mixed assumed-strain finite element model, Mathematics and Mechanics of Solids, 2018, Vol. 23(1) 99 –119, DOI:10.1177/1081286516666405

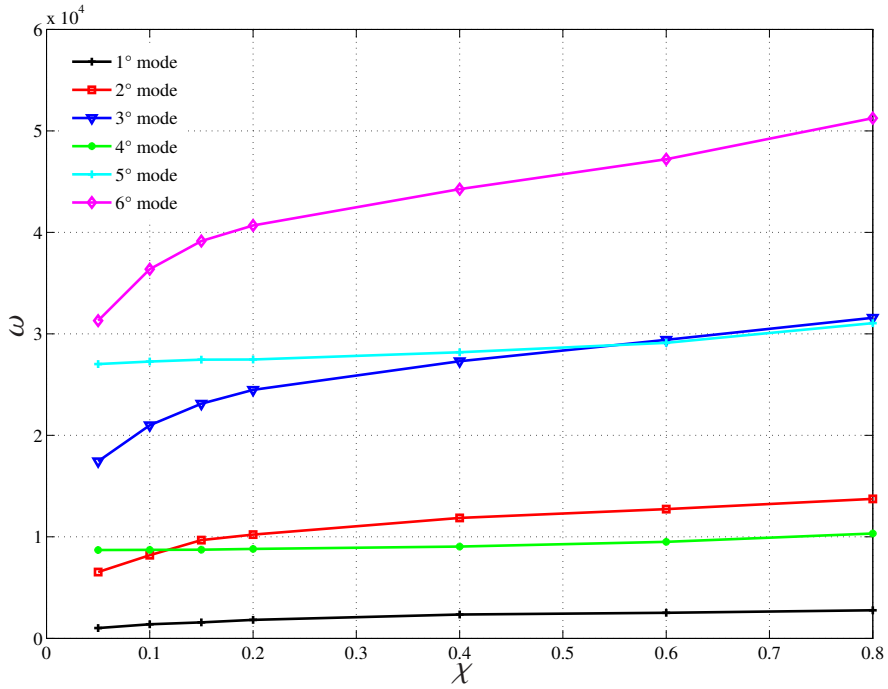

(a) Thick plate: $L/h = 20$

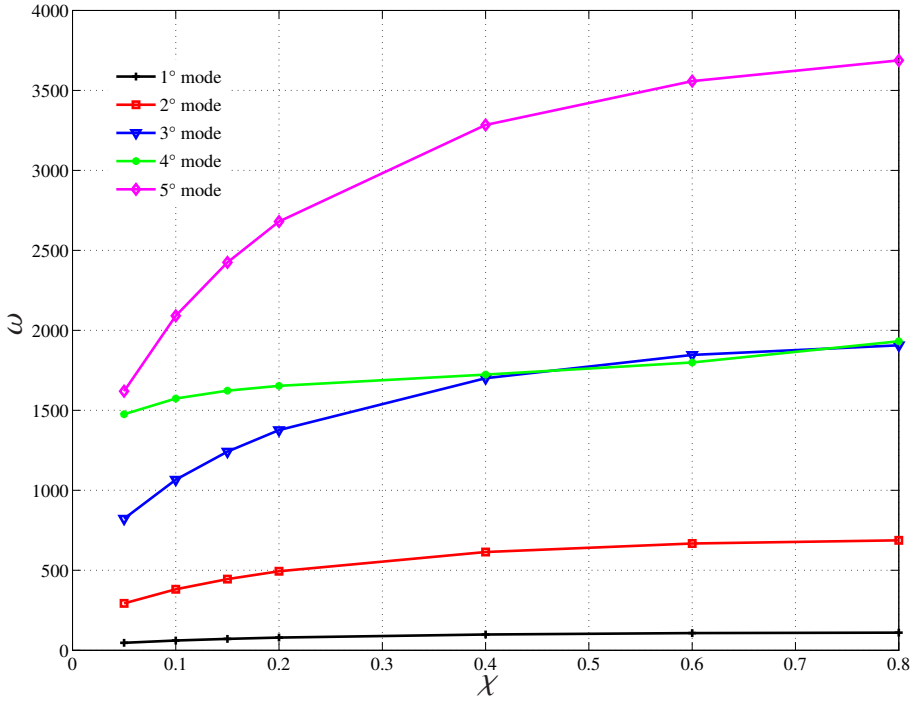

(b) Thin plate: $L/h = 100$

FIGURE 8. Natural frequencies ω for CLP $[0/90]_s$ *vs.* different values of the outer layer thickness ratio χ.

Please cite this document as: Cazzani, Rizzi, Stochino and Turco Modal analysis of laminates by a mixed assumed-strain finite element model, Mathematics and Mechanics of Solids, 2018, Vol. 23(1) 99 –119, DOI:10.1177/1081286516666405

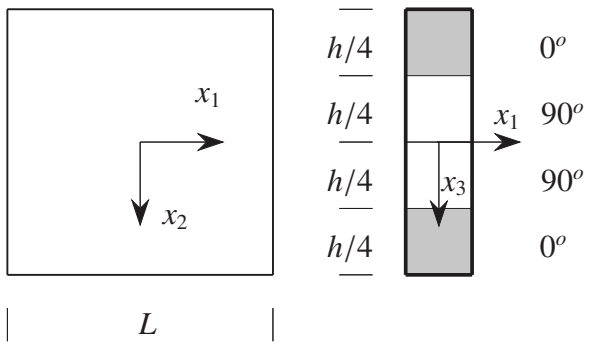

FIGURE 9. Simply supported laminated plate: geometry and orientation of laminae.

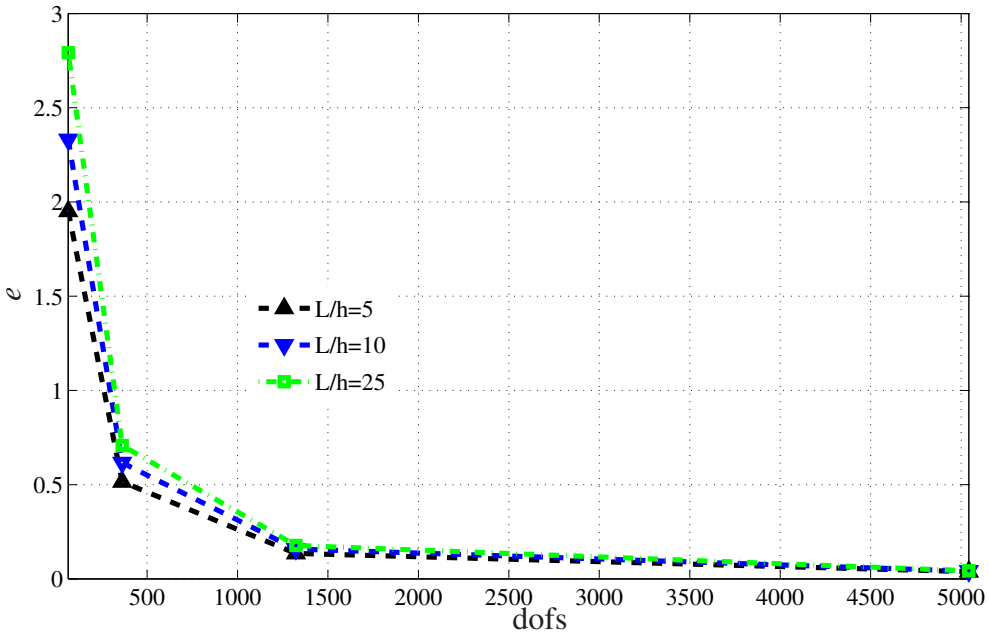

FIGURE 10. Relative error (in percentage) between MAS fundamental frequency and the value provided by FSDT for SSLP *vs.* number of dofs.

Please cite this document as: Cazzani, Rizzi, Stochino and Turco Modal analysis of laminates by a mixed assumed-strain finite element model, Mathematics and Mechanics of Solids, 2018, Vol. 23(1) 99 –119, DOI:10.1177/1081286516666405

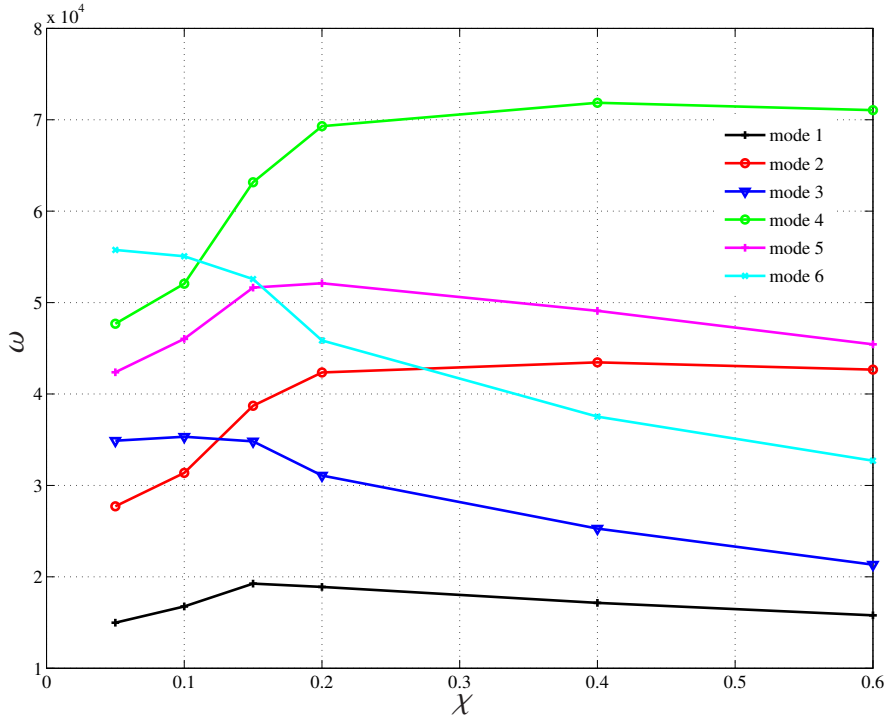

(a) Thick plate: $L/h = 10$

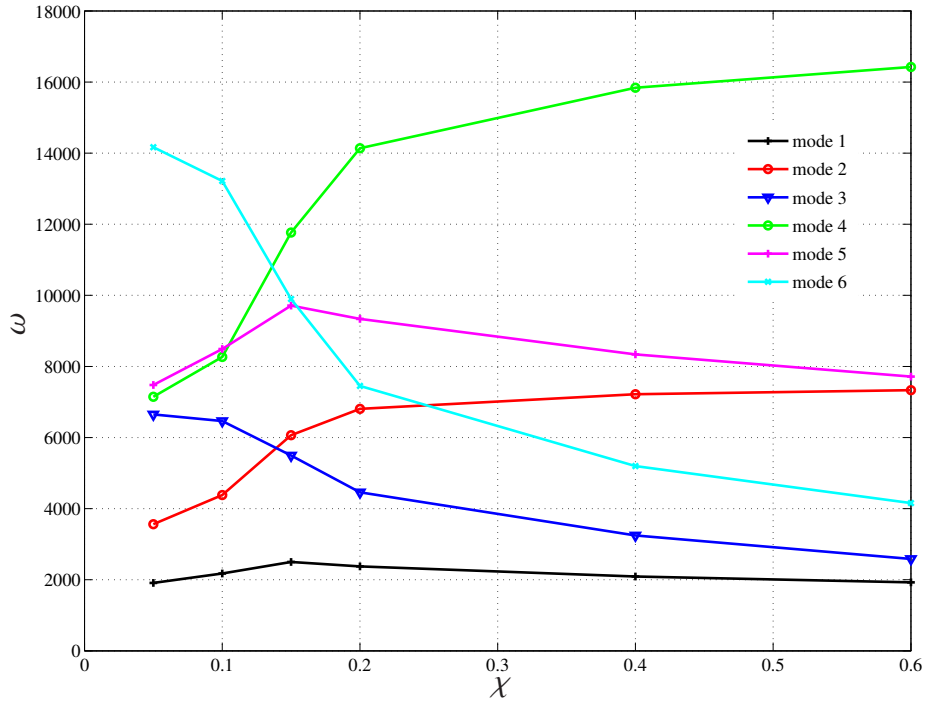

(b) Thin plate: $L/h = 100$

FIGURE 11. Natural frequencies variations ω for SSLP [0°/90°] *vs.* different values of first layer thickness χ.

Please cite this document as: Cazzani, Rizzi, Stochino and Turco Modal analysis of laminates by a mixed assumed-strain finite element model, Mathematics and Mechanics of Solids, 2018, Vol. 23(1) 99 –119, DOI:10.1177/1081286516666405

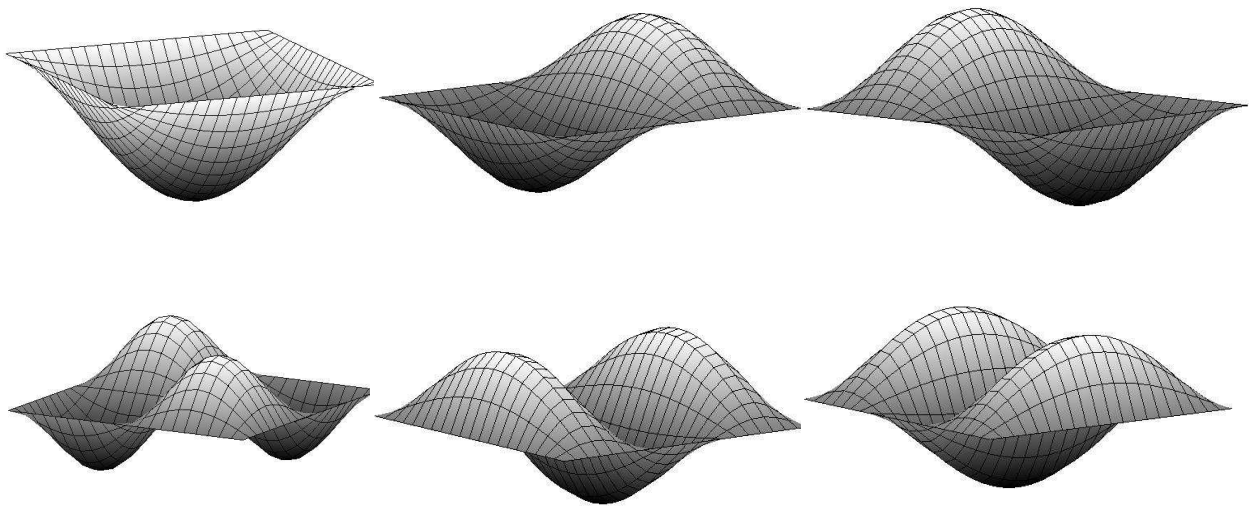

FIGURE 12. Mode shapes corresponding to the first natural frequencies of the SSLP in the case $L/h = 100$ (thin plate) and $\chi = 0.10$.

Please cite this document as: Cazzani, Rizzi, Stochino and Turco Modal analysis of laminates by a mixed assumed-strain finite element model, Mathematics and Mechanics of Solids, 2018, Vol. 23(1) 99 –119, DOI:10.1177/1081286516666405